International Journal of Solids and Structures 48 (2011) 1301–1310

Contents lists available at ScienceDirect

International Journal of Solids and Structures

journal homepage: www.elsevier.com/locate/ijsolstr

Large deformation and stability of an extensible elastica with an unknown length

A. Humer *, H. Irschik

Institute of Technical Mechanics, Johannes Kepler University, Altenberger Str. 69, A-4040 Linz, Austria

ARTICLE INFO

Article history:
Received 10 November 2010
Received in revised form 13 January 2011
Available online 20 January 2011

Keywords:
Extensible elastica
Variable length
Large deformation
Critical load
Constitutive modeling

ABSTRACT

A beam resting on spatially fixed supports may slide relatively to these as soon as external forces are applied. Consequently, the length of the portion of the reference configuration, which is currently located between the supports, depends on the loading and therefore is not known in advance. In the present paper, the problem of a slender beam under a uniformly distributed force is investigated, which is clamped at one side but may slide through another clamping device in axial direction at the opposite side. In combination with a suitable coordinate transformation by which the numerical treatment is simplified, a finite element approach is utilized to determine the equilibrium shape for the maximum critical load that can be imposed on the beam. In the course of this, the influence of the extensibility of the beam axis is studied. A theory based on Reissner's geometrically exact relations for the plane deformation of beams is adapted such that it allows constitutive relations on stress–strain level to be integrated consistently. In addition to the classical equations of the extensible elastica, a constitutive model derived from the St. Venant–Kirchhoff material of non-linear continuum mechanics is studied. The results obtained in this survey are finally compared to those from the linear beam theory, which turns out to be incapable of describing the problem under consideration in a satisfactory manner.

1. Introduction

In the context of rod-like structures, the term stability often refers to problems of buckling, in which the equilibrium path may bifurcate as soon as the applied load exceeds a critical value. An extensive overview on various aspects of this topic is provided in Simitses and Hodges (2006). In the present work, a problem of bending is investigated in which a critical load can also be found, but—in contrast to buckling—equilibrium does not exist beyond this load. Consider a beam, which is clamped at the left-hand side and has another clamping device applied at the right-hand side at a spatially fixed point. This device allows the beam to slide through freely in axial direction but inhibits the rotation of the cross-section currently located there, see Fig. 1. Briefly speaking, the beam may slip out of an orifice at the right side as soon as forces are applied to it. The length of that part of the beam which is currently situated in between the two clamping devices depends on the applied forces and therefore is not known in advance. Neither is the cross-section which is currently located at the clamping device on the right-hand side. Examples for settings of this type include, for instance, hot and cold rolling processes in metal forming.

In literature, problems of this kind are sometimes referred to as variable-arc-length beams (Chucheepsakul et al., 1995). A boundary setting as described above, however, has not been reported so far. Most of the preceding work deals with beams for which one end is hinged while the other one may slide freely over a frictionless point support. For this type of boundaries, beams subjected to terminal couples (Chucheepsakul et al., 1995, 1994, 1999), as well as concentrated forces, both in a fixed direction (Wang et al., 1997) and as a follower force (Chucheepsakul and Phungpaigram, 2004), have been investigated by the research group of Chucheepsakul. More recently, the studies have been extended to the static and dynamic behavior of beams under self-weight, which have been analyzed both analytically and experimentally (Pulngern et al., 2005b,a). A slightly modified boundary setting with one support elevated above the other has been investigated by Athisakul and Chucheepsakul (2008). The stability of a beam under a concentrated force, which is clamped at one end while sliding over a point support at the other, has been studied by Zhang and Yang (2005). The slip-through of a beam under self-weight resting on two point supports has been examined by Chen et al. (2010). With the particular choice of boundary conditions in the present paper, the part of the beam in between the clamping devices is fully decoupled from the outside part without any idealizing assumptions being necessary, in contrast to those cases, in which the beam slides over a point support. A similar setting can be found in the contribution by Ro et al. (2010) on the vibration and stability of a beam with variable length under a compressive force, for which the buckling is constrained by walls parallel to the undeformed beam axis. For a closely related problem, in which the position of an intermediate support with respect to the

* Corresponding author. Tel.: +43 732 2469 6309; fax: +43 732 2469 6282.
E-mail address: alexander.humer@jku.at (A. Humer).

0020-7683/$ - see front matter © 2011 Elsevier Ltd. All rights reserved.
doi:10.1016/j.ijsolstr.2011.01.015

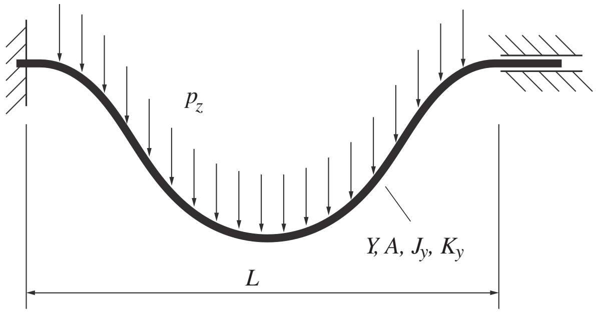

Fig. 1. Deformed configuration of a beam under a uniformly distributed load, which is clamped at the left side and may slide in axial direction at the right side.

reference configuration is unknown whereas its length is known, a dynamic stability analysis has been performed by Spelsberg-Korspeter et al. (2008).

Except for the last reference, in which a linearized beam theory is utilized, the cited work exclusively deals with the large deformation of slender beams for which shear deformation can be ignored. Moreover, only bending deformation is accounted for, which means that the beam axis is assumed to be inextensible. Originating in the ideas of Euler and Kirchhoff (e.g. Love, 1944), beams of this kind are frequently referred to as classical elastica. Likewise, slender beams which may undergo large deformation are considered in the present paper. In contrast to the aforementioned contributions, however, the assumption of axial in-extensibility is not introduced in the following, and the effects resulting from the extensibility on the critical load and the equilibrium shape will be discussed. To this end, a theory based on Reissner's geometrically exact relations for the plane deformation of beams possibly undergoing finite-strain (Reissner, 1972) is adopted. Though shear deformation has also been accounted for by Reissner, it is disregarded in the present work. Particularly, an interpretation of Reissner's strain measures and stress resultants in terms of quantities of non-linear continuum mechanics is utilized, which has recently been presented by Irschik and Gerstmayr (2009). By virtue of this foundation, it is possible to include constitutive relations on the stress–strain level, which allows a large variety of material models to be incorporated consistently into the beam theory. In addition to the extensible elastica, for which both the bending moment and the normal force are proportional to the bending strain and normal force strain, respectively, the St. Venant–Kirchhoff material (SVK) of non-linear continuum mechanics is investigated in the present work. This—still rather simple—type of material behavior already yields a non-linear coupling of bending and axial deformation in the stress resultants. It turns out that the critical load is effectively influenced as soon as axial force strain becomes relevant.

The present paper is organized as follows: in the first section, the material (Lagrangian) representation of the kinematic relations of the beam is introduced and the corresponding deformation gradient is derived. Afterwards, it is shortly outlined how the strain measures and stress resultants in Reissner's theory can be identified by comparing his variational formulation with the principle of virtual work of non-linear continuum mechanics, in which the first Piola–Kirchhoff stress tensor is used as the work-conjugate of the deformation gradient. The stress resultants are presented for two different constitutive models, whereupon the variational formulation of the problem under consideration is provided. The field equations, which can be derived from the variational formulation, are given afterwards, complemented by the appropriate boundary conditions. In the following section, the problem of the unknown length of the reference configuration, which depends on the external load imposed on the beam, is addressed and a coordinate transformation is presented, by which the numerical implications of the unknown length can be avoided elegantly. The effects of the coordinate transformation on the previously introduced quantities and equations are discussed and the modified principle of virtual work is given. After having laid down an appropriate representation of the boundary value problem, the finite element formulation is illustrated briefly and the solution strategy is explained. With the aid of this formulation, approximate solutions for the problem under consideration can be obtained and the results are presented in a non-dimensional framework. In particular, the critical load factor, beyond which no stable equilibrium exists, is determined for different beam geometries and the influence of the respective constitutive behavior is illustrated.

2. Basic equations

In the present section, some relations between structural mechanics and continuum mechanics formulations for beams with large displacements and displacement gradients, as given by Irschik and Gerstmayr (2009), are shortly reviewed and extended.

2.1. Kinematics

Prior to the mathematical description of the geometry of deformation, some basic prerequisites and assumptions need to be introduced. Subsequently, a Cartesian frame $(\boldsymbol{e}_x, \boldsymbol{e}_y, \boldsymbol{e}_z)$ is employed, the x-axis of which coincides with the straight axis of the beam under consideration in the undeformed configuration. Further, the present study is confined to beams which are slender enough for Euler's and Bernoulli's hypothesis to be valid, i.e. throughout the process of deformation, cross-sections originally perpendicular to the axis in the undeformed configuration remain perpendicular, as well as plane and undistorted. In addition, the deformation induced by external forces is assumed to take place in the xz-plane only, see Fig. 2.

Identifying the current position of a material point of the beam axis with the vector $\boldsymbol{r}_0(X)$, the position vector of a point which has initially been at the distance Y and Z to the axis, hence at $\boldsymbol{X} = X\boldsymbol{e}_x + Y\boldsymbol{e}_y + Z\boldsymbol{e}_z$, may be written as

$$\boldsymbol{r}(\boldsymbol{X}) = \boldsymbol{r}_0(X) + Y\boldsymbol{e}_y + Z\boldsymbol{e}_n(X). \tag{1}$$

In the deformed configuration, the cross-sections are rotated by the angle $\varphi(X)$ about the y-axis relative to the undeformed state. Therefore, the unit vector perpendicular to the current axis, which is denoted by $\boldsymbol{e}_n$, is obtained from

$$\boldsymbol{e}_n = \boldsymbol{e}_x \sin\varphi + \boldsymbol{e}_z \cos\varphi. \tag{2}$$

Accordingly, the unit vector tangential to the current axis $\boldsymbol{e}(X)$ becomes

$$\boldsymbol{e} = \boldsymbol{e}_x \cos\varphi - \boldsymbol{e}_z \sin\varphi. \tag{3}$$

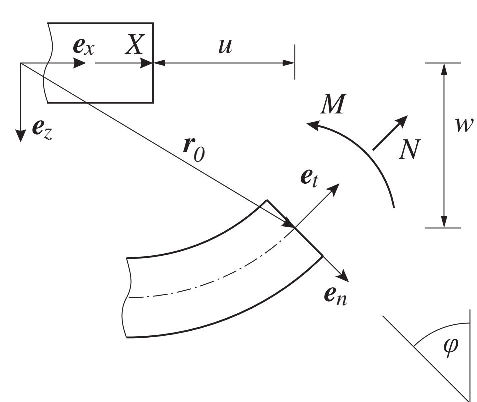

Fig. 2. Kinematics of a Bernoulli–Euler beam.

The tangent unit vector is used to express the derivative of the position vector of a material point of the axis, which is known to be coaxial, as

$$\frac{\partial \mathbf{r}_0}{\partial X} = \boldsymbol{r}'_0 = \Lambda_0 \boldsymbol{e}_t, \tag{4}$$

where Λ_0 is the ratio of the length of a material line element of the axis in the deformed and in the undeformed configuration. Primes are used to indicate the derivative with respect to the axial coordinate X for the sake of brevity.

With the previous relations provided, the deformation gradient $\mathbf{F}(\boldsymbol{X})$ takes the following form:

$$\begin{aligned}\mathbf{F} = \mathrm{Grad}\boldsymbol{r} = (\Lambda_0 + Z\varphi')\cos\varphi \boldsymbol{e}_x \otimes \boldsymbol{e}_x + \sin\varphi \boldsymbol{e}_x \otimes \boldsymbol{e}_z \\ + \boldsymbol{e}_y \otimes \boldsymbol{e}_y - (\Lambda_0 + Z\varphi')\sin\varphi \boldsymbol{e}_z \otimes \boldsymbol{e}_x + \cos\varphi \boldsymbol{e}_z \otimes \boldsymbol{e}_z.\end{aligned} \tag{5}$$

According to the polar decomposition theorem, the deformation gradient may be decomposed uniquely into $\mathbf{F} = \mathbf{RU}$, where $\mathbf{R}$ is an orthogonal rotation tensor and $\mathbf{U} = \mathbf{U}^{\mathrm{T}}$ is the symmetric and positive definite right stretch tensor. By inspecting Eq. (5), one immediately finds, that

$$\begin{aligned}\mathbf{R} = \cos\varphi \boldsymbol{e}_x \otimes \boldsymbol{e}_x + \sin\varphi \boldsymbol{e}_x \otimes \boldsymbol{e}_z + \boldsymbol{e}_y \otimes \boldsymbol{e}_y - \sin\varphi \boldsymbol{e}_z \otimes \boldsymbol{e}_x \\ + \cos\varphi \boldsymbol{e}_z \otimes \boldsymbol{e}_z,\end{aligned} \tag{6}$$

as well as,

$$\mathbf{U} = (\Lambda_0 + Z\varphi')\boldsymbol{e}_x \otimes \boldsymbol{e}_x. \tag{7}$$

In physical terms, $\mathbf{U}$ represents a state of pure stretch along three orthogonal axes, and its eigenvalues are called the principal stretches. Indeed, the principal axes coincide with the Cartesian coordinate system $(\boldsymbol{e}_t, \boldsymbol{e}_y, \boldsymbol{e}_n)$. For this reason, $\Lambda_0 + Z\varphi'$ is the principal stretch of a material line element parallel to the beam axis in the reference configuration, and Λ_0 may consequently be referred to as principal stretch of the axis. After being stretched, the line elements undergo a rotation which is described by the rotation tensor $\mathbf{R}$. Thus, the following relations hold for the unit vectors $\boldsymbol{e}_n$ and $\boldsymbol{e}_t$, Eqs. (2) and (3):

$$\boldsymbol{e}_n = \mathbf{R}\boldsymbol{e}_z, \quad \boldsymbol{e}_t = \mathbf{R}\boldsymbol{e}_x. \tag{8}$$

In order to find approximate solutions, a finite element formulation based on nodal displacements and derivatives of the displacements as degrees of freedom is utilized in the present paper, see Section 4 below. Due to the kinematical assumptions, the three-dimensional problem is reduced to finding the displacement field of the beam axis $\boldsymbol{u}_0$, which is defined as

$$\boldsymbol{u}_0(X) = \boldsymbol{r}_0(X) - X\boldsymbol{e}_x = u(X)\boldsymbol{e}_x + w(X)\boldsymbol{e}_z. \tag{9}$$

The components u and w are referred to as axial displacement and deflection, respectively. In terms of these, the principal stretch Λ_0 can be expressed as

$$\Lambda_0 = \|\boldsymbol{r}'_0\| = \sqrt{(1+u')^2 + w'^2}. \tag{10}$$

Bearing in mind that $\boldsymbol{r}'$ is tangential to the axis, the following equation relates the angle φ to the displacement vector:

$$\varphi = -\arctan\frac{w'}{1+u'}. \tag{11}$$

For later use, the derivative of the angle is also given here:

$$\varphi' = -\frac{(1+u')w'' - w'u''}{\Lambda_0^2}. \tag{12}$$

2.2. Stress resultants and constitutive modeling

According to Reissner (1972), the virtual work of the internal forces of a beam of the length l may be written as

$$\delta W^{int} = \int_l (N\delta\varepsilon + M\delta\kappa)\mathrm{d}X, \tag{13}$$

where $N(X)$ and $M(X)$ denote the normal force and the bending moment. In this expression, $\varepsilon(X)$ and $\kappa(X)$ are the corresponding generalized strain measures, and δ indicates their variations. In order to attach a continuum mechanics interpretation to these quantities, Eq. (13) is compared with the virtual work formulation of non-linear continuum mechanics, see Irschik and Gerstmayr (2009). In the present paper, the virtual work of an arbitrary material volume V is expressed in terms of the deformation gradient $\mathbf{F}$ and the first Piola–Kirchhoff stress tensor $\mathbf{P}$ as its work-conjugate:

$$\delta W^{int} = \int_V \mathbf{P} : \delta\mathbf{F}\,\mathrm{d}V. \tag{14}$$

From Eq. (5), the variation of the deformation gradient is obtained as

$$\begin{aligned}\delta\mathbf{F} = [\delta\Lambda_0\cos\varphi + Z\delta(\varphi')\cos\varphi - (\Lambda_0 + Z\varphi')\delta\varphi\sin\varphi]\boldsymbol{e}_x \otimes \boldsymbol{e}_x \\ + \delta\varphi\cos\varphi \boldsymbol{e}_x \otimes \boldsymbol{e}_z - [\delta\Lambda_0\sin\varphi + Z\delta(\varphi')\sin\varphi \\ + (\Lambda_0 + Z\varphi')\delta\varphi\cos\varphi]\boldsymbol{e}_z \otimes \boldsymbol{e}_x - \delta\varphi\sin\varphi \boldsymbol{e}_z \otimes \boldsymbol{e}_z.\end{aligned} \tag{15}$$

Substituting into Eq. (14) and evaluating the double tensor contraction yields

$$\begin{aligned}\delta W^{int} = \int_l \int_A \{P_{xx}[\delta\Lambda_0\cos\varphi + Z\delta(\varphi')\cos\varphi - (\Lambda_0 + Z\varphi')\delta\varphi\sin\varphi] \\ + P_{xz}\delta\varphi\cos\varphi - P_{zx}[\delta\Lambda_0\sin\varphi + Z\delta(\varphi')\sin\varphi \\ + (\Lambda_0 + Z\varphi')\delta\varphi\cos\varphi] - P_{zz}\delta\varphi\sin\varphi\}\mathrm{d}A\mathrm{d}X,\end{aligned} \tag{16}$$

where the volume integral has been split into two integrals over the cross-section and the length of the beam, respectively. For further simplification, the symmetry condition of the first Piola–Kirchhoff stress tensor,

$$\mathbf{PF}^{\mathrm{T}} = \mathbf{FP}^{\mathrm{T}}, \tag{17}$$

is utilized, from which one finds that

$$P_{xz}\cos\varphi - P_{zz}\sin\varphi = P_{xx}(\Lambda_0 + Z\varphi')\sin\varphi + P_{zx}(\Lambda_0 + Z\varphi')\cos\varphi. \tag{18}$$

Inserting this relation into Eq. (16) renders

$$\begin{aligned}\delta W^{int} = \int_l \int_A [(P_{xx}\cos\varphi - P_{zx}\sin\varphi)\delta\Lambda_0 \\ + Z(P_{xx}\cos\varphi - P_{zx}\sin\varphi)\delta(\varphi')]\mathrm{d}A\mathrm{d}X.\end{aligned} \tag{19}$$

Comparing term by term the structure of this equation with Reissner's formulation, Eq. (13), one can identify the generalized normal force strain as

$$\varepsilon = \Lambda_0 - 1, \tag{20}$$

and the bending strain as

$$\kappa = \varphi'. \tag{21}$$

Analogously, the corresponding stress resultants, i.e. the normal force and the bending moment, are recognized as

$$N = \int_A (P_{xx}\cos\varphi - P_{zx}\sin\varphi)\mathrm{d}A, \tag{22}$$

$$M = \int_A Z(P_{xx}\cos\varphi - P_{zx}\sin\varphi)\mathrm{d}A. \tag{23}$$

A few remarks should be added here for the sake of completeness. The bending strain κ, Eq. (21), is not the geometric curvature of the beam axis, because the derivative of the angle is not taken with respect to the current arc-length, but instead with respect to the referential arc-length X, see Gerstmayr and Irschik (2008) for a discussion. The stress resultants Eqs. (22) and (23) can be visualized recalling the meaning of the components of the first Piola–Kirchhoff stress tensor, which is depicted in Fig. 3. In the Cartesian coordinate system introduced, P_{xx} and P_{zx} are the components of the Lagrangian stress vector $\boldsymbol{s}_x$ acting at a point of a cross-section that has been perpendicular to the beam axis in the reference configuration. The stress resultants, however, are formed by integration of the components of the stress perpendicular to the cross-section in the deformed state. Projecting the stress vector onto the beam axis and utilizing Eq. (3), one may write

$$N = \int_A (\boldsymbol{s}_x \cdot \boldsymbol{e}_t) \mathrm{d}A = \int_A \left(\mathbf{R}^{\mathrm{T}} \boldsymbol{s}_x\right) \cdot \boldsymbol{e}_x \, \mathrm{d}A = \int_A \left(\mathbf{R}^{\mathrm{T}} \mathbf{P} \boldsymbol{e}_x\right) \cdot \boldsymbol{e}_x \, \mathrm{d}A, \tag{24}$$

for the normal force, and

$$M = \int_A Z(\boldsymbol{s}_x \cdot \boldsymbol{e}_t) \mathrm{d}A = \int_A Z\left(\mathbf{R}^{\mathrm{T}} \boldsymbol{s}_x\right) \cdot \boldsymbol{e}_x \, \mathrm{d}A = \int_A Z\left(\mathbf{R}^{\mathrm{T}} \mathbf{P} \boldsymbol{e}_x\right) \cdot \boldsymbol{e}_x \, \mathrm{d}A, \tag{25}$$

for the bending moment. The tensor $\mathbf{T} = \mathbf{R}^{\mathrm{T}}\mathbf{P}$ in the above equations is referred to as Biot stress tensor, for the axial component of which one obtains

$$T_{xx} = P_{xx} \cos\varphi - P_{zx} \sin\varphi. \tag{26}$$

In extension to the linear relations used in the theory of the extensible elastica, Reissner (1973) introduced constitutive equations, which may be non-linear and take the form

$$N = N(\varepsilon, \kappa) \tag{27}$$

and

$$M = M(\varepsilon, \kappa), \tag{28}$$

in the Bernoulli–Euler case. Although a large variety of material behavior may be described by this means, staying in the context of structural mechanics, Reissner (1973) suggested to experimentally identify the constitutive relations. With the continuum mechanics foundation provided in this section, it is possible to incorporate material behavior on the stress–strain level into the beam theory, see Eqs. (22) and (23). In the present derivation, the first Piola–Kirchhoff stress tensor has been utilized. An alternative approach based on the second Piola–Kirchhoff stress tensor has been presented by Irschik and Gerstmayr (2009). Moreover, if beam geometries are considered, for which the influence of shear deformation cannot be neglected, similar relations can be found, see Irschik and Gerstmayr (2011) for an extension of the relations above.

First, the constitutive behavior of the extensible elastica is studied. To this end, the definition of the Biot strain tensor is recalled, which is related to the right stretch tensor by $\mathbf{H} = \mathbf{U} - \mathbf{I}$. Assuming a linear relation between the Biot stress and strain,

$$\mathbf{T} = \mathbf{C}^B : \mathbf{H}, \tag{29}$$

in which $\mathbf{C}^B$ denotes the fourth-order elastic modulus tensor, one obtains the following constitutive equation for the uni-axial state of strain considered here:

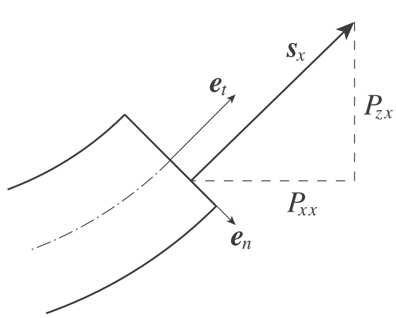

Fig. 3. The Lagrangian stress vector $\boldsymbol{s}_x$ and its components.

$$T_{xx} = Y^B H_{xx} = Y^B(\Lambda_0 + Z\varphi' - 1). \tag{30}$$

The material constant Y^B denotes the C^B_{xxxx} component of $\mathbf{C}^B$. If the beam under consideration is homogenous and the beam axis is chosen in such a way that the first moment of area of the cross-sections vanishes,

$$\int_A Z \, \mathrm{d}A = 0, \tag{31}$$

integration over the cross-section in Eqs. (24) and (25) can be performed, from which one obtains

$$N = Y^B A(\Lambda_0 - 1) = Y^B A \varepsilon, \tag{32}$$

by utilizing Eq. (26), as well as

$$M = Y^B J_y \varphi' = Y^B J_y \kappa, \tag{33}$$

where J_y denotes the second moment of area,

$$J_y = \int_A Z^2 \, \mathrm{d}A. \tag{34}$$

The above relations provide a continuum mechanics interpretation of the theory of the extensible elastica, in which no coupling between the strain measures emerges in the stress resultants.

This, however, changes with the second constitutive relation under consideration. For a material of the St. Venant–Kirchhoff type, the second Piola–Kirchhoff stress tensor $\mathbf{S}$ depends linearly on the Green strain tensor $\mathbf{E}$, i.e. $\mathbf{S} = \mathbf{C}^S : \mathbf{E}$, with the elastic modulus tensor being denoted by $\mathbf{C}^S$ here. The first and the second Piola–Kirchhoff stress tensor are related by means of

$$\mathbf{S} = \mathbf{F}^{-1}\mathbf{P} = \mathbf{U}^{-1}\mathbf{R}^{\mathrm{T}}\mathbf{P}, \tag{35}$$

where the orthogonality property of the rotation tensor $\mathbf{R}^{\mathrm{T}} = \mathbf{R}^{-1}$ has been used. From the definition of the Green strain tensor,

$$\mathbf{E} = \frac{1}{2}(\mathbf{U}^2 - \mathbf{I}), \tag{36}$$

the general form of the constitutive equation is obtained as

$$\mathbf{R}^{\mathrm{T}}\mathbf{P} = \frac{1}{2}\mathbf{U}[\mathbf{C}^S : (\mathbf{U}^2 - \mathbf{I})]. \tag{37}$$

With the kinematical assumptions of the present beam theory, this may be reduced to the following scalar equation,

$$P_{xx} \cos\varphi - P_{zx} \sin\varphi = \frac{1}{2} Y^S (\Lambda_0 + Z\varphi') \left[(\Lambda_0 + Z\varphi')^2 - 1\right], \tag{38}$$

in which the material constant is denoted by $Y^S = C^S_{xxxx}$. From Eq. (22), the normal force follows as

$$\begin{aligned} N &= \frac{1}{2} Y^S \Lambda_0 \left[A(\Lambda_0^2 - 1) + 3J_y \varphi'^2\right] \\ &= Y^S \left[A\varepsilon\left(\frac{1}{2}\varepsilon^2 + \frac{3}{2}\varepsilon + 1\right) + J_y \frac{3}{2}(\varepsilon + 1)\kappa^2\right], \end{aligned} \tag{39}$$

and the bending moment is obtained from Eq. (23) as

$$\begin{aligned} M &= \frac{1}{2} Y^S \kappa \left(K_y \kappa^2 + 3J_y \Lambda_0^2 - J_y\right) \\ &= Y^S \left[K_y \frac{1}{2}\kappa^3 + J_y \kappa \left(\frac{3}{2}\varepsilon^2 + 3\varepsilon + 1\right)\right]. \end{aligned} \tag{40}$$

Obviously, the constitutive relations of both the normal force and the bending moment Eqs. (39) and (40) exhibit a non-linear coupling of bending strain and axial strain. Besides, the fourth-order moment of area appears in (40), which is denoted by K_y, with

$$K_y = \int_A Z^4 \, \mathrm{d}A. \tag{41}$$

The St. Venant–Kirchhoff law, however, suffers from the drawback that large compressive strains E_{xx} can be reached by finite stresses, which constitutes an unphysical behavior. Nevertheless, the St. Venant–Kirchhoff material law has proven to be worthwhile in those frequent cases, in which the Green strains are small, but the deformation gradients are large. In such a situation, the linearized expressions for strain would yield erroneously large values of strain. In Humer and Irschik (2009), a hyperelastic material based on ideas by Palmov (1998) has been presented.

2.3. Variational formulation and equilibrium relations

According to the principle of virtual work, the virtual work of the internal forces δW^{int} is balanced by the virtual work of the external forces δW^{ext}. In the present paper, only uniformly distributed loads are considered. Let p_x and p_z denote the components of the force vector per unit undeformed length in the horizontal and vertical direction, $\boldsymbol{p} = p_x \boldsymbol{e}_x + p_z \boldsymbol{e}_z$, then the virtual work of the external forces is given by

$$\delta W^{ext} = \int_l \boldsymbol{p} \cdot \delta \boldsymbol{u} \, dX = \int_l (p_x \delta u + p_z \delta w) dX. \tag{42}$$

Consequently, the principle of virtual work reads

$$\delta W^{int} - \delta W^{ext} = \int_l (N\delta\varepsilon + M\delta\kappa - p_x\delta u - p_z\delta w) dX = 0. \tag{43}$$

Analogously to Reissner (1972), the local form of the balance equations and the corresponding boundary conditions are obtained from the variational formulation Eq. (43) by substituting the virtual changes of the strain measures appropriately and subsequent integration by parts. For a detailed derivation, refer to Irschik and Gerstmayr (2009). Although the problem is treated by the aid of a finite element approach, which is based on the variational formulation, the local form of balance equation is given here for the sake of completeness:

$$N' + \frac{M'}{\Lambda_0}\varphi' + n = 0, \tag{44}$$

$$\varphi' N - \left(\frac{M'}{\Lambda_0}\right)' - q = 0. \tag{45}$$

In these equations, n and q denote the components of the load vector represented in the local coordinate system, whose axes are tangential and perpendicular to the beam axis, thus $\boldsymbol{p} = n\boldsymbol{e}_t + q\boldsymbol{e}_n$. Consequently, they are obtained with the aid of the rotation tensor $\mathbf{R}$ as

$$n = p_x \cos\varphi - p_z \sin\varphi \tag{46}$$

and

$$q = p_x \sin\varphi + p_z \cos\varphi. \tag{47}$$

In addition to the variational formulation and the equilibrium equations, boundary conditions need to be specified prior to seeking solutions of the problem. At its left-hand side, see Fig. 1, the beam is clamped, which means that both the displacement of the axis and the rotation of the cross-section are prohibited. At the right-hand side, however, the beam may slide out of the orifice without resistance from friction or other processes. Consequently, it is assumed that the normal force and the deflection at the material point, which is currently located there, do vanish. Moreover, the rotation of the cross-section belonging to this point of the axis is hindered by the clamping device. Formally, the boundary conditions read

$$X = 0: \quad u(X=0) = 0, \quad w(X=0) = 0, \quad \varphi(X=0) = 0 \tag{48}$$

and

$$X = l: \quad w(X=l) = 0, \quad \varphi(X=l) = 0, \quad N(X=l) = 0. \tag{49}$$

3. Unknown length of the reference configuration

One could think that the problem under consideration is fully determined by either the variational formulation Eq. (43) or the local field equations Eqs. (44) and (45) supplemented by the particular constitutive relations and the boundary conditions. Yet, this is not the case, since it has tacitly been assumed in the previous derivations that the length l of the beam is known a priori. As the beam may slide out due to the imposed load, the length of the reference configuration of the beam that is currently located between the two boundaries is not known. Neither is the material point at which the boundary conditions on the right-hand side are to be applied. Correspondingly, one may write

$$l = L + \Delta L, \tag{50}$$

in which L is the known distance between the supports, whereas the length ΔL of the additional portion still is to be determined.

From the numerical point of view, various solution strategies are imaginable. As previously stated, finite elements are subsequently used to find approximate solutions. For this method, an obvious possibility would be to utilize a sufficiently long beam, then generate the mesh, and finally solve the problem by iteratively adapting both the point at which the boundary conditions are applied and the region subjected to the external forces. The convergence behavior of such an approach, however, would be rather poor most probably, because the position of the boundary conditions would not coincide with the location of the nodes in general. In order to circumvent this problem, the mesh would have to be regenerated in each iteration. Moreover, a larger amount of elements—and therefore degrees of freedom—than actually necessary would have to be utilized. An elegant way of avoiding these issues is provided by the following coordinate transformation. Let ξ denote a new axial coordinate, which is related to the material coordinate X by

$$\xi = \frac{L}{L + \Delta L} X, \tag{51}$$

then the domain in which a solution has to be found becomes $\xi \in [0, L]$ instead of the previously variable domain $X \in [0, L + \Delta L]$, whose right boundary depends on the external forces. A transformation of that kind has also been used by Vu-Quoc and Li (1995) for investigations on the dynamics of an axially sliding beam, for which, however, the length l is variable yet known at all times. The transformation (51) is linear in the material coordinate X since it represents a mere scaling by a still unknown factor, for which the abbreviation

$$\gamma = \frac{L}{L + \Delta L}, \tag{52}$$

is utilized. Each physical quantity of a material point represented by a function—be it scalar-, vector-, or tensor-valued—of the coordinate X may be expressed in terms of the new coordinate ξ by

$$f(X) = f(X(\xi)) = \bar{f}(\xi(X)) = \bar{f}(\xi), \tag{53}$$

where an over-bar is used to indicate the change in the argument of the function. The chain-rule of differential calculus renders

$$f'(X) = \frac{\partial \bar{f}(\xi)}{\partial \xi}\frac{\partial \xi}{\partial X} = \frac{\partial \bar{f}(\xi)}{\partial \xi}\gamma = \bar{f}'(\xi)\gamma, \tag{54}$$

for the first derivative with respect to X of the function $f(X)$, and accordingly

$$f^{(n)}(X) = \frac{\partial^n \bar{f}(\xi)}{\partial \xi^n} \gamma^n, \tag{55}$$

for the nth derivative. A prime on a transformed function is used to indicate the derivative with respect to ξ. With these transformation rules at hand, it is possible to express the previously introduced equations—in particular the field Eqs. (44) and (45) as well as the variational formulation Eq. (43)—in terms of the new coordinate ξ. For the latter, which represents the foundation of the finite element formulation to be used here, one obtains

$$\int_0^L \left(\overline{N}\delta\bar{\varepsilon} + \overline{M}\delta\bar{\kappa} - \bar{p}_x\delta\bar{u} - \bar{p}_z\delta\bar{w}\right)\gamma^{-1}\,\mathrm{d}\xi = 0. \tag{56}$$

Note that, in contrast to Eq. (43), the domain of integration in the transformed representation Eq. (56) is known in advance. The boundary conditions Eqs. (48) and (49) are also prescribed at fixed positions with respect to ξ, which do not vary with the applied load:

$$\xi = 0: \quad \bar{u}(\xi = 0) = 0, \quad \bar{w}(\xi = 0) = 0, \quad \bar{\varphi}(\xi = 0) = 0 \tag{57}$$

and

$$\xi = L: \quad \bar{w}(\xi = L) = 0, \quad \bar{\varphi}(\xi = L) = 0, \quad \overline{N}(\xi = L) = 0. \tag{58}$$

The finite element formulation utilized in the present work is based on displacement degrees of freedom only. Consequently, in Eq. (56), the stress resultants, which in turn depend on the strain measures, and the variations of the strain measures have to be expressed in terms of the transformed components of the displacement vector. For the normal force strain, one finds

$$\bar{\varepsilon} = \bar{\Lambda}_0 - 1 = \sqrt{(1+\bar{u}'\gamma)^2 + (\bar{w}'\gamma)^2} - 1, \tag{59}$$

as well as

$$\delta\bar{\varepsilon} = \gamma\frac{(1+\bar{u}'\gamma)\delta\bar{u}' + \bar{w}'\delta\bar{w}'\gamma}{\bar{\Lambda}_0}, \tag{60}$$

for its first variation. Analogously, the transformed bending strain reads

$$\bar{\kappa} = \bar{\varphi}'\gamma = -\gamma^2\frac{(1+\bar{u}'\gamma)\bar{w}'' - \bar{w}'\bar{u}''\gamma}{\bar{\Lambda}_0^2}, \tag{61}$$

from which the variation is obtained as

$$\delta\bar{\kappa} = 2\gamma^3\frac{[(1+\bar{u}'\gamma)\bar{w}'' - \bar{w}'\bar{u}''\gamma][(1+\bar{u}'\gamma)\delta\bar{u}' + \bar{w}'\delta\bar{w}'\gamma]}{\bar{\Lambda}_0^4} - \gamma^2\frac{\bar{w}''\delta\bar{u}'\gamma - \bar{u}''\delta\bar{w}'\gamma + (1+\bar{u}'\gamma)\delta\bar{w}'' - \bar{w}'\delta\bar{u}''\gamma}{\bar{\Lambda}_0^2}. \tag{62}$$

The problem under consideration is not fully determined, since the scaling factor γ in the transformation involves the additional length ΔL, which still is unknown. In order to close the set of equations, a relation for ΔL has to be provided. It is immediately recognized that ΔL equals the negative axial displacement of the material point of the axis which is currently located at the boundary on the right side. The missing relation therefore reads

$$\Delta L = -u(X = L + \Delta L) = -\bar{u}(\xi = L). \tag{63}$$

4. Numerical considerations and examples

Due to the non-linearity of the equations, closed-form solutions of the extensible elastica can only be found for a few particular load cases and boundary settings. Formulated with the angle φ as independent variable, the governing equation of a thin rod, which is held and bent by terminal forces and couples, can be identified with the equation of motion of a rigid pendulum according to Kirchhoff's kinetic analogue (Love, 1944). Therefore, solutions can sometimes be found in terms of elliptic integrals, see for example Bisshopp and Drucker (1945) for the bending of an inextensible cantilever. More recently, the buckling of an extensible elastica has been investigated by Magnusson et al. (2001).

As soon as distributed forces are involved, the situation becomes more complicated, since then closed-form solutions do not exist for large deformations. For a uniformly distributed vertical load, the term heavy elastica is used, as the weight of the structure represents the probably most prominent load case. A review on the extensive literature on the heavy elastica and the various numerical methods applied to it is given by Wang (1986). The solution strategies range from polynomial expansions, see for instance the early work by Rohde (1953), to various finite element schemes. A special finite element formulation, which takes the unknown length of the reference configuration into account, is developed and outlined shortly in what follows.

4.1. Finite element formulation

The variational formulation Eq. (56) can be written in the following fixed-point form,

$$F(\bar{\boldsymbol{u}}, \delta\bar{\boldsymbol{u}}) = 0, \tag{64}$$

which is non-linear in the displacement $\bar{\boldsymbol{u}}$ and linear in the virtual displacement $\delta\bar{\boldsymbol{u}}$. In order to find an approximate solution, Newton's iteration is applied, which requires the non-linear form Eq. (64) to be linearized. In the present work, the linearization is performed in the continuous domain prior to discretization. Let

$$DF(\Delta\bar{\boldsymbol{u}}, \delta\bar{\boldsymbol{u}}) = \lim_{s\to 0}\left[\frac{\mathrm{d}}{\mathrm{d}s}F(\bar{\boldsymbol{u}} + s\Delta\bar{\boldsymbol{u}}, \delta\bar{\boldsymbol{u}})\right], \tag{65}$$

denote the directional derivative of the non-linear form $F(\bar{\boldsymbol{u}}, \delta\bar{\boldsymbol{u}})$ with respect to the displacement—a bi-linear form in the increments of the displacement $\Delta\bar{\boldsymbol{u}}$ and the virtual displacements $\delta\bar{\boldsymbol{u}}$—then the linearized problem reads

$$DF(\Delta\bar{\boldsymbol{u}}, \delta\bar{\boldsymbol{u}}) = -F(\bar{\boldsymbol{u}}, \delta\bar{\boldsymbol{u}}). \tag{66}$$

A finite element method based on displacement degrees of freedom is utilized. One also refers to this type of approach, in which no rotational degrees of freedom are used, as absolute nodal coordinate formulation. The components of the (transformed) displacement vector, $\bar{u}$ and $\bar{w}$, as well as their first and second spatial derivatives, $\bar{u}'$, $\bar{w}'$, $\bar{u}''$ and $\bar{w}''$ represent the degrees of freedom of a node. Consequently, an element with two nodes possesses twelve degrees of freedom, which may be gathered in the vector of element coordinates $\boldsymbol{q}$,

$$\boldsymbol{q} = \left[\bar{u}_1\bar{w}_1\bar{u}_1'\bar{w}_1'\bar{u}_1''\bar{w}_1''\bar{u}_2\bar{w}_2\bar{u}_2'\bar{w}_2'\bar{u}_2''\bar{w}_2''\right]^{\mathrm{T}}, \tag{67}$$

where the index distinguishes the left node (1) from the right one (2). Pursuing the matrix notation, one may express the interpolation of the displacement vector in terms of the shape function matrix $\mathbf{\Sigma}$ and the degrees of freedom of an element as

$$\bar{\boldsymbol{u}} = \mathbf{\Sigma}\boldsymbol{q}. \tag{68}$$

The shape functions $S_1,\ldots,S_6$ are organized in the shape function matrix in such a way that

$$\mathbf{\Sigma} = [S_1\mathbf{I} \quad S_2\mathbf{I} \quad S_3\mathbf{I} \quad S_4\mathbf{I} \quad S_5\mathbf{I} \quad S_6\mathbf{I}], \tag{69}$$

where $\mathbf{I}$ denotes the 2×2 unit matrix. For the independence of the coordinates, fifth-order polynomials are required for the interpolation, which are given as follows for an element of the length L:

$$S_1 = 1 - 10\left(\frac{\xi}{L}\right)^3 + 15\left(\frac{\xi}{L}\right)^4 - 6\left(\frac{\xi}{L}\right)^5, \tag{70}$$

$$S_2 = \frac{\xi}{L} - 6\left(\frac{\xi}{L}\right)^3 + 8\left(\frac{\xi}{L}\right)^4 - 3\left(\frac{\xi}{L}\right)^5, \tag{71}$$

$$S_3 = \frac{1}{2}\left(\frac{\xi}{L}\right)^2 - \frac{3}{2}\left(\frac{\xi}{L}\right)^3 + \frac{3}{2}\left(\frac{\xi}{L}\right)^4 - \frac{1}{2}\left(\frac{\xi}{L}\right)^5, \tag{72}$$

$$S_4 = 10\left(\frac{\xi}{L}\right)^3 - 15\left(\frac{\xi}{L}\right)^4 + 6\left(\frac{\xi}{L}\right)^5, \tag{73}$$

$$S_5 = -4\left(\frac{\xi}{L}\right)^3 + 7\left(\frac{\xi}{L}\right)^4 - 3\left(\frac{\xi}{L}\right)^5, \tag{74}$$

$$S_6 = \frac{1}{2}\left(\frac{\xi}{L}\right)^3 - \left(\frac{\xi}{L}\right)^4 + \frac{1}{2}\left(\frac{\xi}{L}\right)^5. \tag{75}$$

For a convenient numerical integration, a normalized coordinate is introduced, which requires a transformed set of Eqs. (70)–(75) to be implemented.

The same interpolation as for the displacement field is chosen for both the displacement increment and the virtual displacement, hence

$$\Delta\bar{\boldsymbol{u}} = \boldsymbol{\Sigma}\Delta\boldsymbol{q}, \tag{76}$$

as well as

$$\delta\bar{\boldsymbol{u}} = \boldsymbol{\Sigma}\delta\boldsymbol{q}. \tag{77}$$

Now, substituting the interpolations Eqs. (68), (76) and (77), the linearized variational formulation Eq. (56) turns into

$$DF(\Delta\boldsymbol{q}, \delta\boldsymbol{q}) = -F(\boldsymbol{q}, \delta\boldsymbol{q}). \tag{78}$$

Performing integration over the element, one obtains the discrete variational formulation, which may be written in matrix notation as

$$\delta\boldsymbol{q}\cdot\mathbf{K}(\boldsymbol{q})\Delta\boldsymbol{q} = \delta\boldsymbol{q}\cdot\boldsymbol{f}(\boldsymbol{q}), \tag{79}$$

which gives a system of twelve linear equations

$$\mathbf{K}(\boldsymbol{q})\Delta\boldsymbol{q} = \boldsymbol{f}(\boldsymbol{q}). \tag{80}$$

In the previous equations, $\mathbf{K}$ and $\boldsymbol{f}$ denote the element stiffness matrix and the load vector, respectively. If the beam is partitioned into n finite elements, the global system of $6n + 6$ equations is formed by assembling the element stiffness matrices and vectors appropriately. Without going into detail, it should be annotated that the geometric boundary conditions are enforced by Lagrange multipliers, by which five equations are added for the setting under investigation.

A few words on the treatment of the additional length ΔL seem to be in order. As previously shown, the problem is closed by introducing the algebraic relation Eq. (63), so that the system of equations could actually be solved directly. Nevertheless, an incremental approach is utilized, in which a converged solution of the displacement field is constructed first keeping ΔL fixed, before the calculation is repeated with an updated ΔL. Although the computational expense seems to increase at the first glance, this solution strategy has proven to be more stable, in particular, as soon as the critical load is approached and convergence becomes critical.

4.2. External forces

In the present study, the probably most natural load case of a uniformly distributed force in vertical direction is investigated. For a homogenous beam, a load of this kind is equivalent to the force originating in the gravitational field, which is proportional to the density of the structure in the reference configuration. The load vector per unit undeformed length then takes a particularly simple form, since the horizontal component vanishes identically, $p_x = 0$, so that

$$\boldsymbol{p} = p_z\boldsymbol{e}, \quad p_z = \text{const}. \tag{81}$$

As it is assumed that the force does not vary throughout the length of the beam, the coordinate transformation Eq. (51) yields

$$\bar{p}_z = p_z = \text{const}. \tag{82}$$

The transformed variational formulation Eq. (56) consequently reads

$$\int_0^L (\overline{N}\delta\bar{\varepsilon} + \overline{M}\delta\bar{\kappa} - p_z\delta\bar{w})\gamma^{-1}\,\mathrm{d}\xi = 0. \tag{83}$$

4.3. Non-dimensional setting

For the sake of generality, the results are presented in a non-dimensional setting. To this end, the span L between the two clamping devices is used for the scaling, i.e. ξ/L is the non-dimensional coordinate in axial direction. Similarly, the transversal deflection and the axial displacement are made non-dimensional by relating them to the span. Hence, one obtains the non-dimensional quantities $\bar{w}/L$ and $\bar{u}/L$.

Pursuing this procedure, two non-dimensional similarity parameters are identified, by which the problem is completely governed. The first parameter, which is denoted by η, provides a relation between the extensional stiffness YA and the bending stiffness YJ_y of the beam:

$$\eta = \frac{YA}{YJ_y}L^2. \tag{84}$$

In case of homogeneous rectangular cross-sections, which are considered here for the sake of simplicity, η is fully determined by the ratio of the height of the cross-section and the span:

$$\eta = 12\left(\frac{L}{h}\right)^2. \tag{85}$$

The second parameter is the non-dimensional load factor λ, which relates the bending stiffness to the external force per unit length:

$$\lambda = \frac{p_zL^3}{YJ_y}. \tag{86}$$

Provided that the beam has to bear its own weight as the only load, λ may be expressed in terms of the density ϱ as

$$\lambda = 12\frac{\varrho gL^3}{Yh^2}, \tag{87}$$

where g denotes the constant of gravitation.

In order to verify the approximate solutions by comparison, the results in Table 2 of Pulngern et al. (2005b), who considered an inextensible elastica, for which one end is hinged, while the other slides over a frictionless point support, have been reproduced to a satisfactory degree using the linear constitutive behavior. A detailed study on the effects of extensibility and non-linear material behavior for this different boundary setting will be conducted in the future.

4.4. Results

With the aid of the numerical method described above, the critical loads and corresponding equilibrium configurations are studied for various beam geometries on the one hand, and for the different types of material behavior on the other hand. To this end, the beam is partitioned into 256 finite elements, which has proven to be sufficient to obtain converged results. In order to determine the maximum force the beam can carry, the load factor λ is gradually increased by a small increment, which in turn is reduced as soon as no equilibrium is found any more. The calculations have been carried out for a number of different beam proportions, starting from height-to-length ratios of 10^{-4} up to 5×10^{-2}. Within this range, the assumption of shear deformation having very little influence is most certainly valid, see for example Ziegler (1998).

In Table 1, the values of the critical load λ_{crit}, the maximum non-dimensional deflection of the corresponding equilibrium configuration $\bar{w}_{crit}/L$, which is found at the mid-span $\xi/L = 1/2$, and the non-dimensional length $\Delta L_{crit}/L$, by which the reference configuration exceeds the span L, are presented for different values of h/L and for both the extensible elastica and the St. Venant–Kirchhoff type material.

First, it is observed that for very slender beams with a small height-to-length ratio, the critical load values as well as equilibrium shape are approximately the same. An explanation can be found in the constitutive relations of the bending moment, Eqs. (33) and (40): for smaller values of h/L, and conversely for an increasing ratio between extensional and bending stiffness η, the beam axis becomes more and more inextensible. For an inextensible beam, which exclusively exhibits bending deformation and for which the axial strain vanishes identically, $\varepsilon = 0$, the expressions for the bending moment Eqs. (33) and (40) resemble closely. The only difference is the third-order term in material curvature κ in the relations of the St. Venant–Kirchhoff material. In the problem under consideration, however, κ is small compared to one, which is why the results are very much alike.

For increasing values of the height-to-length ratio, the two different types of constitutive modeling feature a reverse characteristic. In case of the extensible elastica, both the critical load factor and the scaled maximum deflection increase with the beam getting thicker compared to its length, whereas the non-dimensional length of the reference configuration decreases. For the St. Venant–Kirchhoff material, the converse behavior is observed, see Fig. 4.

Chucheepsakul et al. (1995) have shown that a second unstable equilibrium configuration exists in case of the previously described beam with hinged ends for each load below the critical value. Each perturbation of such a configuration, in which the deflection exceeds the deflection at the critical load, induces the beam to slide out infinitely. With the finite element approach employed here, it has not been possible to find unstable configurations in the present setting. Provided these do exist, a shooting method as presented by Chucheepsakul et al. (1994) could be utilized for the detection.

Finally, the results of the geometrically exact relations presented above are compared to those obtained from a beam theory of lower order. The first-order non-linear strain–displacement relation is obtained from Eq. (20) by a binomial series expansion as

$$\varepsilon \approx u' + \frac{1}{2}(w')^2. \tag{88}$$

The angle φ is approximated by the negative derivative of the deflection,

$$\varphi \approx -w', \tag{89}$$

from which the material curvature simply follows as

$$\kappa \approx -w''. \tag{90}$$

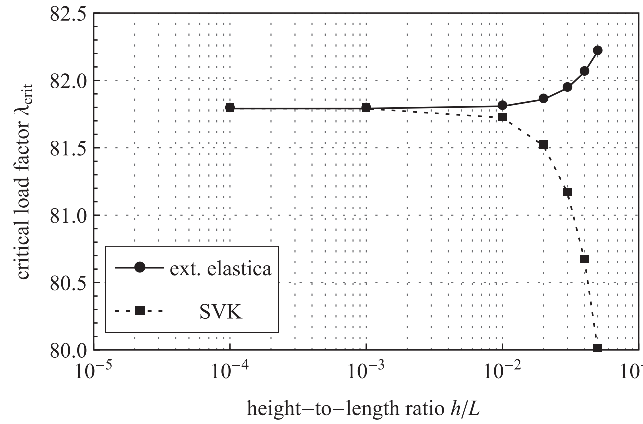

Fig. 4. Comparison of the critical load factor λ_{crit} of the extensible elastica and the St. Venant–Kirchhoff type material on a logarithmic scale.

Similar to the extensible elastica, the normal force and the bending moment are proportional to the (approximate) axial strain and the (approximate) curvature. For the present problem, the governing differential equations then follow from a variational principle (Simitses and Hodges, 2006) as

$$N' = 0, \tag{91}$$

$$(Nw' + M')' + p_z = 0. \tag{92}$$

Since $N(X = L + \Delta L) = 0$ holds at the right boundary, the normal force and the axial strain vanish in the whole domain, hence $N = 0$ and $\varepsilon = 0$. Eq. (92) is reduced to the first-order beam theory, i.e.

$$w'''' = \frac{p_z}{YJ_y}, \tag{93}$$

which may be integrated immediately. Considering the boundary conditions, $w(X = 0) = 0$, $w(X = L + \Delta L) = 0$, $w''(X = 0) = 0$, and $w''(X = L + \Delta L) = 0$, one finds

$$w = \frac{p_z(L + \Delta L - X)^2 X^2}{24YJ_y}. \tag{94}$$

As the strain ε is zero, the axial displacement is obtained from Eq. (88)

$$u = -\frac{p_z^2 X^3 \left(70l^4 - 315l^3X + 546l^2X^2 - 420lX^3 + 120X^4\right)}{60480(YJ_y)^2}, \tag{95}$$

where $l = L + \Delta L$ is used again for the sake of brevity. Recalling Eq. (63), the following relation between the external load p_z and the additional length ΔL is established:

$$\Delta L = \frac{p_z^2(L + \Delta L)^7}{60480(YJ_y)^2}. \tag{96}$$

From this equation, the critical load factor may be determined symbolically as

Table 1
Critical load factor, maximum deflection, and additional length for various beam geometries.

h/L	λ_{crit}		$\bar{w}_{crit}(\xi = 0.5L)/L$		$\Delta L_{crit}/L$	
	Ext. elastica	SVK	Ext. elastica	SVK	Ext. elastica	SVK
1×10^{-4}	81.7912943	81.7912858	0.4207480	0.4207561	0.3726535	0.3726660
1×10^{-3}	81.7914615	81.7906093	0.4207558	0.4207553	0.3726633	0.3726644
1×10^{-2}	81.8081813	81.7228531	0.4208395	0.4205884	0.3725805	0.3723673
2×10^{-2}	81.8588854	81.5161912	0.4210927	0.4200392	0.3723279	0.3714035
3×10^{-2}	81.9435193	81.1671184	0.4215113	0.4191191	0.3719004	0.3698028
4×10^{-2}	82.0622741	80.6680568	0.4221002	0.4176383	0.3713039	0.3672923
5×10^{-2}	82.2154184	80.0068343	0.4228484	0.4154332	0.3705191	0.3636531

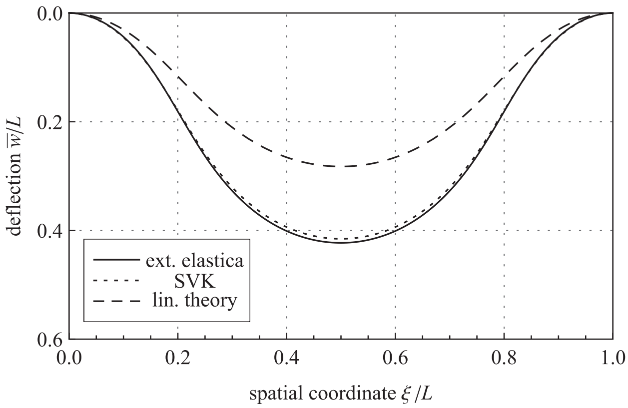

Fig. 5. Comparison of the equilibrium shapes of the extensible elastica, the St. Venant–Kirchhoff model, and the linear theory for a height-to-length ratio of $h/L = 5 \times 10^{-2}$ at the respective critical load.

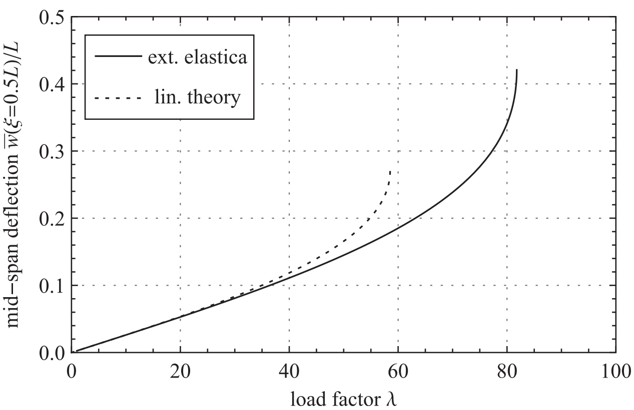

Fig. 6. Comparison of the mid-span deflection of the extensible elastica and the linear theory for a height-to-length ratio of $h/L = 1 \times 10^{-3}$.

$$\lambda_{crit} = \frac{5184}{343}\sqrt{15}. \tag{97}$$

Based on this result, the corresponding non-dimensional values of the maximum deflection, and the additional length are found:

$$\frac{w_{crit}}{L} = \frac{7}{32}\sqrt{\frac{5}{3}}, \quad \frac{\Delta L_{crit}}{L} = \frac{1}{6}. \tag{98}$$

As a consequence of the vanishing normal force, the behavior of the beam is not influenced by the extensional stiffness since only bending deformation is relevant.

In Fig. 5, the equilibrium configurations at the respective critical load of the geometrically exact relations and the linear beam theory are compared. The linear relations obviously fail to capture the behavior of the beam correctly as the maximum deflection is significantly smaller. Moreover, it can be seen that for comparably thick beams the constitutive modeling does have a notable influence on the equilibrium shape.

Fig. 6 shows the relation of the non-dimensional mid-span deflection to the load factor. For small values of λ, the linear theory agrees with the geometrically exact relations. With an increasing load, however, the behavior diverges more and more, and it finally turns out that the critical load obtained the linear beam theory is roughly 71% of the critical load found with the non-linear theory.

5. Concluding remarks

In the present work, the critical load and the equilibrium configuration of a slender beam with an unknown length of the reference configuration under a uniformly distributed load have been investigated. The study has been performed utilizing a geometrically exact beam theory based on Reissner's relations for the case of a plane deformation. The constitutive relations of both the extensible elastica and the St. Venant–Kirchhoff type have been incorporated by establishing a connection between the strain measures and stress resultants of the beam theory and of non-linear continuum mechanics. In order to conveniently find approximate solutions using a finite element formulation, a coordinate transformation has been introduced, by which the problem of non-material boundary conditions has been circumvented. Besides the two different types of elastic material behavior, the influence of the axial extensibility has been examined in the present study. It has been shown that within the range, in which the Bernoulli–Euler assumptions are valid, the axial deformation indeed affects the critical load and the corresponding equilibrium configuration of the beam. Finally, a comparison of the exact relations with the linear beam theory has shown that the latter fails to represent the behavior of the beam correctly.

Acknowledgments

The authors gratefully acknowledge the support of the Comet K2 Austrian Center of Competence in Mechatronics (ACCM).

References

Athisakul, C., Chucheepsakul, S., 2008. Effect of inclination on bending of variable-arc-length beams subjected to uniform self-weight. Eng. Struct. 30 (4), 902–908.
Bisshopp, K.E., Drucker, D.C., 1945. Large deflection of cantilever beams. Quart. Appl. Math. 3 (3), 272–275.
Chen, J.S., Li, H.C., Ro, W.C., 2010. Slip-through of a heavy elastica on point supports. Int. J. Solids Struct. 47 (2), 261–268.
Chucheepsakul, S., Buncharoen, S., Huang, T., 1995. Elastica of simple variable-arc-length beam subjected to end moment. J. Eng. Mech. 121 (7), 767–772.
Chucheepsakul, S., Buncharoen, S., Wang, C.M., 1994. Large deflection of beams under moment gradient. J. Eng. Mech. 120 (9), 1848–1860.
Chucheepsakul, S., Phungpaigram, B., 2004. Elliptic integral solutions of variable-arc-length elastica under an inclined follower force. Z. Angew. Math. Mech. 84 (1), 29–38.
Chucheepsakul, S., Wang, C.M., He, X.Q., Monprapussorn, T., 1999. Double curvature bending of variable-arc-length elasticas. J. Appl. Mech. 66 (1), 87–94.
Gerstmayr, J., Irschik, H., 2008. On the correct representation of bending and axial deformation in the absolute nodal coordinate formulation with an elastic line approach. J. Sound. Vib. 318, 461–487.
Humer, A., Irschik, H., 2009. Large deflections of beams with an unknown length of the reference configuration. in: Proc. 50th AIAA/ASME/ASCE/AHS/ASC Structures, Structural Dynamics, and Materials Conf., Palm Springs, CA, 04–07 May 2009, Paper No. 2009–2371.
Irschik, H., Gerstmayr, J., 2009. A continuum mechanics based derivation of Reissner's large-displacement finite-strain beam theory: the case of plane deformations of originally straight Bernoulli–Euler beams. Acta Mech. 206 (1-2), 1–21.
Irschik, H., Gerstmayr, J., 2011. A continuum-mechanics interpretation of reissner's non-linear shear-deformable beam theory. Math. Comput. Mod. Dyn. Syst. 17 (1), 19–29.
Love, A.E.H., 1944. A Treatise on the Mathematical Theory of Elasticity, 4th ed. Dover Publications Inc, New York.
Magnusson, A., Ristinmaa, M., Ljung, C., 2001. Behaviour of the extensible elastica solution. Int. J. Solids Struct. 38 (46–47), 8441–8457.
Palmov, V.A., 1998. Vibrations of Elasto-Plastic Bodies [translated by A. Belyaev]. Springer Verlag, Berlin, Heidelberg.
Pulngern, T., Chucheepsakul, S., Halling, M.W., 2005a. Analytical and experimental studies on the large amplitude free vibrations of variable-arc-length beams. J. Vib. Control 11 (7), 923–947.
Pulngern, T., Halling, M.W., Chucheepsakul, S., 2005b. Large deflections of variable-arc-length beams under uniform self weight: analytical and experimental. Struct. Eng. Mech. 19 (4), 413–424.
Reissner, E., 1972. On one-dimensional finite-strain beam theory: the plane problem. Z. Angew. Math. Phys. 23 (5), 795–804.
Reissner, E., 1973. On one-dimensional large-displacement finite-strain beam theory. Stud. Appl. Math. 52, 87–95.
Ro, W.C., Chen, J.S., Hong, S.Y., 2010. Vibration and stability of a constrained elastica with variable length. Int. J. Solids Struct. 47 (16), 2143–2154.
Rohde, F., 1953. Large deflections of a cantilever beam with uniformly distributed load. Quart. Appl. Math. 11, 337–338.
Simitses, G.J., Hodges, D.H., 2006. Fundamentals of Structural Stability. Elsevier.

Spelsberg-Korspeter, G., Kirillov, O.N., Hagedorn, P., 2008. Modeling and stability analysis of an axially moving beam with frictional contact. J. Appl. Mech. 75 (3), 31001-1–31001-10.
Vu-Quoc, L., Li, S., 1995. Dynamics of sliding geometrically-exact beams: large angle maneuver and parametric resonance. Comput. Methods Appl. Mech. Eng. 120 (1–2), 65–118.
Wang, C.M., Lam, K.Y., He, X.Q., Chucheepsakul, S., 1997. Large deflections of an end supported beam subjected to a point load. Int. J. Non Linear Mech. 32 (1), 63–72.
Wang, C.Y., 1986. A critical review of the heavy elastica. Int. J. Mech. Sci. 28 (8), 549–559.
Zhang, X., Yang, J., 2005. Inverse problem of elastica of a variable-arc-length beam subjected to a concentrated load. Acta Mech. Sin. 21 (5), 444–450.
Ziegler, F., 1998. Mechanics of Solids and Fluids, 2nd ed. Springer, New York.